Image Anal Stereol 2001;20:225-229
Original Research Paper

ROUGHNESS CHARACTERIZATION OF AN INDOOR ENVIRONMENT

NISRINE DOUIRI, MAJDI KHOUDEIR AND CHRISTIAN OLIVIER
IRCOM-SIC, UMR-CNRS n° 6615, 86962 Futuroscope-Chasseneuil Cedex, France
e-mail: Douiri@sic.sp2mi.univ-poitiers.fr
(Accepted October 29, 2001)

ABSTRACT

For a transmission at 60 GHz inside the buildings, the models of propagation currently developed do not take into account the 3D roughness of surfaces under consideration. In this paper, we deal with the evaluation of the 3D roughness of surfaces in this kind of environment. An indoor environment includes different types of surfaces but the most representative of 3D roughness are walls, ceiling and floor. We propose a method to characterise the 3D roughness of these surfaces by constructing an image space made up of the original image, the image of gradient, the image of curvature and the image of the angles between the perpendicular to the grey level surface and the perpendicular to the whole image. The method we have developed is based, first, on the study of correlation variations of our image space, and second on a frequency analysis of the angle image histograms. The elaborated criteria allowed us to classify the surfaces studied.

Keywords: classification, grey level texture, image space, indoor environment and roughness.

INTRODUCTION

Due to the huge development in telecommunications, the operators of communication networks have to improve their techniques in order to use the frequency spectrum more efficiently. Thus, they have improved the intelligence in the systems through the concept of frequency re-use (Cichon and Wiesbeck, 1994). That has led to mobile cellular radio communication systems such as the GSM (900 MHz), the DCS 1800 (1800 MHz) and the recent UMTS, which represents the new generation of mobile system. At the same time, to enable a high rate data transmission inside buildings by Hertzian channel, studies are being carried out to optimize the phenomena of transmission at 60 GHz. Thus, the corresponding wavelength is in millimeters. At this frequency, it is important for the operators to have information related to physical characteristics and surface nature of the walls encountered during the transmission. The models of propagation of radio electric waves, currently developed for an indoor environment, do not take into account the 3D roughness of surfaces and the intrinsic properties of materials.

To optimize the models of radioelectric wave propagation inside buildings, we propose to evaluate the 3D roughness of the main reflection surfaces. An indoor environment includes different types of walls: the room walls, the ceiling, the floor and the furniture surfaces. If we consider roughness, room walls are more representative of an indoor environment than furniture surfaces. For this reason, we analyse in a first stage, 3D roughness of wall, floor and ceiling. Thus we consider four room walls with different degrees of roughness (Fig. 1a-d), a portion of ceiling (Fig. 1e), and a floor covering of fitted carpet (Fig. 1f). The local relief of these walls has an average height varying from 1 - 5 mm. The surfaces studied can be considered as stochastic textures. The images of these surfaces are taken with a gray level camera. The conditions of the shots are chosen in order to obtain, on one hand, a sufficient resolution (one pixel = 0.9 mm²) to emphasize the local relief of the walls, and on the other hand, to have optimal conditions for illuminant (Chantler, 1995).

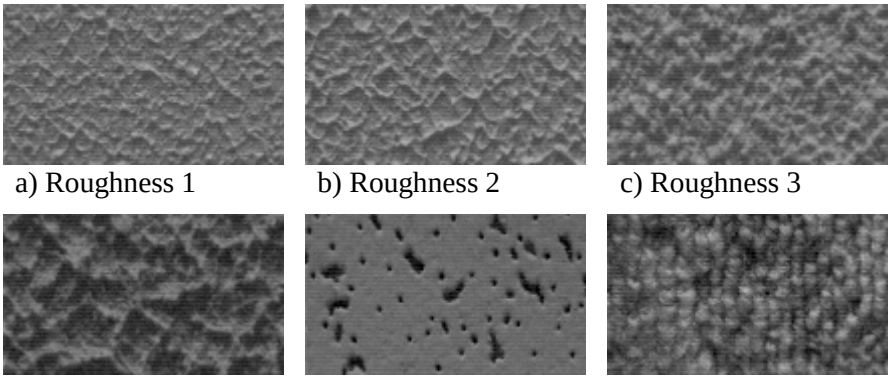

a) Roughness 1 b) Roughness 2 c) Roughness 3

d) Roughness 4 e) Roughness 5 f) Roughness 6

Fig. 1. *Samples of indoor environment surfaces.*

SUGGESTED METHODS

In optics, the intensity *I* received by the camera sensor can be expressed by:

$$I = L\frac{\cos\alpha}{r^2} \quad \text{or} \quad I = \frac{L}{\sqrt{1+\left(\frac{\partial Z}{\partial x}\right)^2+\left(\frac{\partial Z}{\partial y}\right)^2}}. \tag{1}$$

The intensity I is therefore a function of the luminance L of the camera sensor, the angle α between the camera axis and the perpendicular to the surface of reflection and the distance *r* between the camera and the surface studied. (*x*, *y*) represent the continuous planar coordinates, and Z is the magnitude of the relief studied.

For a surface of uniform colour, the variations of gray levels in the image can be representative of the variations of relief Z. The different types of surfaces we have studied in an indoor environment correspond to this assumption.

CONSTRUCTION OF AN IMAGE SPACE

We consider therefore that the variations of gray levels in the image correspond to a great extent to the variations of the relief. So first, we propose to define a set of images highlighting the variations of curvatures in the image. Our image space will be made up of the original image, the image of gradient, the image of curvature and the image of the angles between the perpendicular to the local gray level surface and the perpendicular to the whole image.

To characterize the original image geometrically, we first studied, a point neighbourhood, which is characterized by the image of gradient (Fig. 2a). Let us consider a random texture whose gray levels are noted $I_{i,j}$ where (*i, j*) designate discrete coordinates. The image of local gradient, noted ΔI, in (*i, j*) can be expressed by:

$$\Delta I(i,j) = \frac{L}{r^2}\left(\left|\cos\alpha_{i,j} - \cos\alpha_{i+1,j}\right| + \left|\cos\alpha_{i,j} - \cos\alpha_{i,j+1}\right|\right), \tag{2}$$

where (*i* + 1, *j*) and (*i, j*+1) are two neighbours of the coordinates (*i, j*) of the point under consideration (Deutsch and Belknap, 1972). In order to take into account the different scales of 3D roughness, the image of the gradients was calculated on different scales. Thus, the gradient image gives access to the amplitude variations of gray levels, and the frequency distribution of these variations.

In order to highlight the curvature variations in the image, we construct first, the image of the angles θ between the perpendicular to the gray level surface and the perpendicular to the whole image. The angle $\theta(i, j)$ in (*i, j*) can be expressed by:

$$\cos\theta(i,j) = \frac{2}{\sqrt{\left(I_{i-1.j} - I_{i+1.j}\right)^2 + \left(I_{i,j-1} - I_{i,j+1}\right)^2 + 4}}. \tag{3}$$

In addition, to take into account a possible texture pattern, we calculate this image on different scales and we consider the four neighbours in different directions of the image.

Then, we make the image of the curvatures from the original image. The surface S of the image is defined locally by a parametric representation: $S(x,y) = (x, y, I(x,y))^T$. The local derivatives of the first and second order of the image are noted $I_x, I_y, I_{xx}, I_{xy}, I_{yy}$. In each point of S, we suppose that the surface is orientated by the perpendicular

vector $\vec{N} = \vec{S}_x \wedge \vec{S}_y$ with $\vec{S}_x = (1,0,I_x)^T$ and $\vec{S}_y = (0,1,I_y)^T$. After applying the first and second fundamental forms, we obtain the principal maximal ρ_{max} and minimal ρ_{min} curvatures of the image surface. Their combination enables us to define the Gaussian curvature and the average curvature. Our aim is to extract information about the three-dimensional relief variations from a two-dimensional image surface. Thus, the variations of average curvature are more significant than those of the Gaussian curvature. For this reason, we used the average curvature ρ_{moy} obtained from the average of the principal curvatures ρ_{max} and ρ_{min} of the image surface. So:

$$\rho_{moy} = \frac{\rho_{\max} + \rho_{\min}}{2} = \frac{(1+I_y^{\,2})I_{xx} - 2I_xI_yI_{xy} + (1+I_x^{\,2})I_{yy}}{2(1+I_x^{\,2}+I_y^{\,2})^{3/2}} \quad (4)$$

We show on Fig. 2b and c respectively the image of the angles and the image of the curvature for room wall of roughness 4.

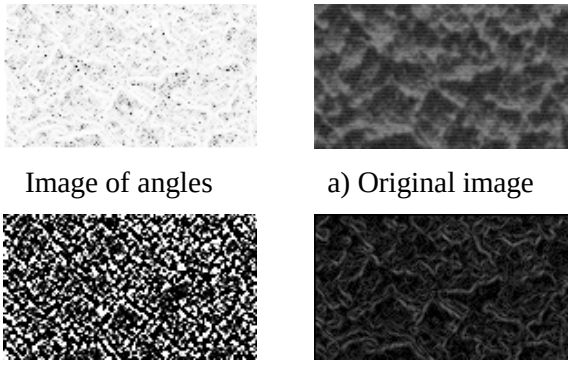

Image of angles a) Original image

b) Image of curvatures c) Image of gradient

Fig. 2. *Sample of image space for mural wall of roughness 4.*

CRITERIA FOR CLASSIFICATION

To classify our textures in terms of 3D relief, we considered as a first criterion, the maximum of the partial gradients of correlation surface: we extracted the slopes from the surface of correlation then calculated their average (King and Spedding, 1983). We fixed a threshold on the image of correlation, checked against the whole of our image bank. The value of the threshold is obtained after computing the gradient of the surface of correlation and corresponds to the coordinates of the maximum value of this gradient. Thus, the first criterion will be expressed by:

$$Crit1 = \max\left(\left|\frac{\partial C(t,s)}{\partial t}\right| + \left|\frac{\partial C(t,s)}{\partial s}\right|\right) \quad (5)$$

where (t,s) are the parameters of translation and C is the correlation surface.

In the first criterion, we used information from partial derivatives. Nevertheless, these partial gradients are sensitive to the surface rotation. At this stage, we add a second criterion based on the main eigenvalues λ of these correlation surfaces C. Although the distributions of gradient vary, the eigenvalues remain unchanged. A classification based on the eigenvalues must be unchanged with rotation (Chantler and McGunnigle, 2000). Consequently, the eigenvalues can be representative of the degree of surface roughness. So, a second criterion is defined:

$$Crit2 = |\textit{main value of eigenvalues } \lambda|. \quad (6)$$

To complete our study, we deal with an analysis of low frequencies of the angle image histograms in order to highlight the variations of curvatures of the 3D relief. A low value of roughness can be reflected in the histograms of the angles by a concentration of occurrences of the angles in the low value areas, and also by a decrease of its standard deviation. Thus, a third criterion can be defined from the standard deviation of the low frequencies of these histograms.

$$Crit3 = \text{var}\,(\textit{histogram } (I_\theta)), \quad (7)$$

where I_θ is the angle image and "var" is the variance of histogram of values I_θ.

RESULTS

We tested these criteria, for each wall, on fifty images of different zones. The values given in figure 3 are the average values of these tests. The three elaborated criteria are applied to our set of images. We represent in Fig. 3 the evolution of these criteria according to wall roughness (1, 2, 3 and 4), ceiling (5) and floor roughness (6). Thus, we observe a rise in the maximum value of the slopes of correlation surface with an increase in the surface roughness (Fig. 3a). The same texture classification is observed overall by the standard deviation values of the low frequency of the angle image histograms (Fig. 3c). We also notice the decrease in the main eigenvalue with an increase in 3D roughness of the surfaces. This decrease of eigenvalues is illustrated in Fig. 3b.

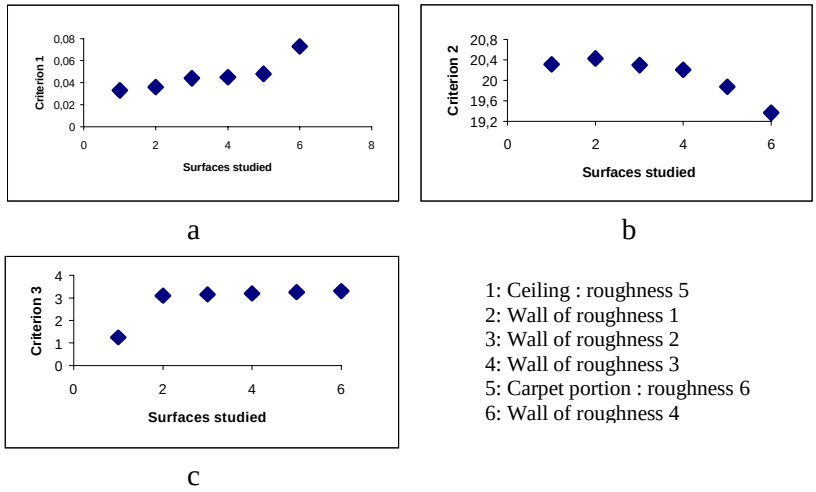

Fig. 3. *Evolution of the criteria according to 3D roughness, a. Evolution of criterion 1, b. Evolution of criterion 2 and c. Evolution of criterion 3.*

These criteria enable us to define a global criterion of 3D roughness based on the first and second order statistics of these criteria. A discriminating vector X defines it by :

$$X = \left[Crit_1(x), Crit_2(x), Crit_3(x)\right].$$

In order to compare the 3D roughness X of a studied surface to 3D roughness of our image bank, we first apply, the three criteria to the image. Then, we compute the Mahalanobis distance between the vector X and the vector $rug(i)$ defined by $\left[(m_1,\sigma_1)(i),(m_2,\sigma_2)(i),(m_3,\sigma_3)(i)\right]$; the values (m_i, σ_i), with $i = 1,2,3$, represent respectively the average value and the standard deviation of the three criteria applied to the roughness i of our image bank. The Mahalanobis distance (Basseville, 1988) between vectors X and $rug(i)$ is expressed by:

$$\begin{aligned} D\left[X, rug(i)\right] = & \frac{1}{\sigma_1(i)}\left[\left(Crit_1(x) - m_1(i)\right)^2\right] \\ & + \frac{1}{\sigma_2(i)}\left[\left(Crit_2(x) - m_2(i)\right)^2\right] \\ & + \frac{1}{\sigma_3(i)}\left[\left(Crit_3(x) - m_3(i)\right)^2\right]. \end{aligned} \quad (8)$$

The Class i of roughness X is selected such that the Mahalanobis distance between the two vectors is minimal. Table 1 shows the obtained results following state x of X.

Table 1. *Evolutions of the Mahalanobis distance according to 3D roughness x.*

Distance values	*roughness 1*	*roughness 2*	*roughness 3*	*roughness 4*	*roughness 5*	*roughness 6*
x ∈ roughness 1	**0.09**	0.48	1.54	12.71	100.17	1.24
x ∈ roughness 2	0.59	**0.05**	0.29	9.39	108.1	0.56
x ∈ roughness 3	1.28	0.30	**0.10**	8.28	113.74	0.35
x ∈ roughness 4	21.02	16.30	16.67	**0.17**	93.78	1.78
x ∈ roughness 5	74.32	47.95	72.17	64.71	**0.23**	44.14
x ∈ roughness 6	12.65	9.47	8.24	5.55	119.15	**0.81**

These results show the difficulty of classifying roughness levels 2 and 3 (see Fig. 3), compared to the 4 others levels.

CONCLUSION

In this paper, we developed a method for the classification of surfaces studied in terms of 3D relief. This method is based, on one hand, on the study of correlation variations of our image space, and on the other hand, on a frequency analysis of the histograms of the image of angle. The application of these criteria to our bank of images allowed a relative classification of the surfaces studied in terms of 3D relief. To finalise our study of indoor environment roughness, we will have to extend our method to colour images. In this case, we will have to separate information related to the colour from information linked to the relief. Then we will be able to characterise textured surfaces in terms of local relief.

REFERENCES

Basseville M (1988). Distance Measures for Signal Processing and Pattern Recognition. INRIA Rapport Interne No.422, Septembre.

Chantler MJ (1995). Why Illumination Direction is Fundamental to Texture Analysis. IEE Proc.-Vis. Image Signal Process 142;4:199-206.

Chantler MJ, McGunnigle G (2000). On The Use of Gradient Space Eigenvalues for rotation invariant texture classification. I.C.P.R 2000, Barcelone, Spain, Sept., 943-6.

Cichon DJ, Wiesbeck W (1994). Ray Optical Wave Propagation Modeling In Urban Micro Cells. 5th IEEE International Symposium on Personal, Indoor and Mobile Radio Communication 94, The Netherlands, September.

Deutsch ES, Belknap NJ (1972). Texture Descriptors Using Neighborhood Information. Computer Graphics Image Processing 1, 145-68.

Deygout J (1991). Correction Factor for Multiple Knife-edge Diffraction. IEEE Trans. on Antennas and Propagation, 39(8), August.

Khoudeir M, Brochard J, Augereau B (2000). Discrimination de Surfaces Texturées 3D: Application à la Caractérisation de l'Usure de Revêtements Routiers. IAPR Vision Interface 2000, Montreal, Canada, 174-8.

King TG, Spedding TA (1983). Towards a Rational Surface Profile Characterization System. Precision Engineering 5(4):153-60.

McGunnigle G, Chantler MJ (2000). Rough Surface Classification Using Point Statistics From Photometric Stereo. Pattern Recognition Letters 21:593-604.

Bajcsy R, Lieberman L (1976). Texture Gradient as a Depth Cue. Computer Graphics and Image Processing 5:52-67.

Stout KJ, Sullivan PJ, Dong WP, Mainsah E, Luo N, Mathia T, Zahouani H (1993). The Developpment of Methods for The Caracterisation of Roughness in Three Dimensions. Phase II Report, No.3374/1/0/170/90/1-BCR, European Community, Brussels, April.